

# An Energy-Based Flight Planning System for Unmanned Traffic Management

Zhilong Liu

Dept. of Civil and Environmental Engineering  
University of California, Berkeley  
Berkeley California 94720, USA  
Email: lz1200102109@berkeley.edu

Raja Sengupta

Dept. of Civil and Environmental Engineering  
University of California, Berkeley  
Berkeley California 94720, USA  
Email: sengupta@ce.berkeley.edu

**Abstract**—In this paper, we proposed an energy-based flight planning system for Unmanned Aircraft Systems (UAS) Traffic Management (UTM). Fuel consumption estimation at the flight planning stage is safety critical in general aviation, because energy-related failures are often life-threatening. However, conservative fuel estimation is not economical and environmentally friendly because carrying unnecessary fuel load burns a lot of extra fuel. The same reasoning holds in UTM. Aviation researchers are actively working on optimizing fuel loading, but such research is lacking in UTM. In this paper, we aim to optimize energy consumption in UTM with a flight planning system. The accuracy and effectiveness of the system is illustrated by experiments and simulations, respectively.

## I. INTRODUCTION

Recent advances in sensing and computing technology has made unmanned aerial systems (UAS) low-cost but increasingly capable of executing complex missions in challenging environments. They have gained popularity in a vast range of civilian applications, including goods delivery, infrastructure surveillance, agricultural monitoring, and photography. To ensure the safe separation between small UAS (sUAS) and the general aviation, the Federal Aviation Administration (FAA) restricts sUAS operations to be in Class G airspace and at low-altitude, or below 500 feet above ground level (AGL) [1]. However, many challenges remain for large-scale sUAS operations to become a reality. First, many applications require sUAS to be operated beyond visual-line-of-sight (VLOS), which imposes safety issues and is prohibited by the FAA right now. Second, the key infrastructure to enable the widespread use of low-altitude airspace and UAS operations does not exist [2]. Therefore, a new research topic called UAS traffic management (UTM) comes into place at the National Aeronautics and Space Administration (NASA) [3]. The NASA UTM program lists many research topics, such as static obstacle avoidance, collision avoidance between vehicles, wind and weather effects, and communication problems. A large subset of these problems can be addressed at the flight planning stage before a flight takes place.

Flight planning is important in UTM. First, it can better protect the general public and reduce the negative externalities from UTM missions. In general aviation, pilots' interest is aligned with the public because small mistakes may cost pilots' lives. However, in UTM failures, the society often bears

much more negative consequences compared to the pilots due to the autonomous nature. A good flight plan before the actual mission helps the pilots foresee and avoid many possible risks and failures, and thus better protect the society. Second, optimal flight planning can reduce the operational costs in UTM missions. For example, energy shortage in missions may force the vehicle to perform emergency landing and introduce huge recycling costs. On the other hand, if vehicles and batteries are frequently over-sized in small missions, the additional operational costs can be significant. Flight plans provide optimal solutions to this dilemma.

In this paper, we would like to propose an energy-based flight planning system for a single multirotor sUAS under the influence of wind and static obstructions. The paper is organized as follows. First, before discussing UTM flight planning, we have to understand how it is performed in the general aviation today. This process is reviewed briefly in Section II. Then, the sUAS flight planning problem is broken into three sub-problems, namely power consumption model identification, optimal routing, and wind estimation. Third, the three sub-problems are addressed in separate sections. Experiments and simulations are presented within each subsection. The wind estimation problem is still in progress, so it will only be introduced conceptually and left as future work.

## II. FLIGHT PLANNING IN GENERAL AVIATION

In general Aviation, an essential part of the flight planning problem is fuel loading. It is generally estimated conservatively, to ensure passenger safety and reduce energy-based contingency cost. For example, fuel deficiency can cause emergency landing in bad weather conditions. On the other hand, fuel accounts for a significant portion of the aircraft weight, and extra fuel weight causes unnecessary fuel burn. To reduce costs and environmental impacts, airlines strive to achieve fuel consumption reduction. Significant research has been performed to evaluate the efficiency of current aviation practice [4], [5]. Similar to other economic problems, fuel loading in aviation is a balance between capacity and demand. The energy capacity is given by the amount of fuel loaded on board. On the other hand, the energy demand is much more involved.

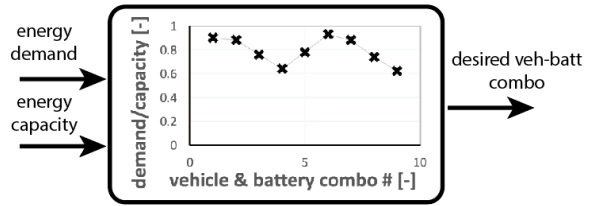
First, the demand computation requires fuel consumption models based on aircraft performance. The fuel consumption computation relies mostly on publicly available data. The majority of this data is a combination of Eurocontrols Base of Aircraft Data (BADA) to calculate fuel consumed while airborne and the International Civil Aviation Organization (ICAO) Engine Exhaust Emissions Data Bank to calculate fuel consumed on the ground [6]. Researchers have also worked on more accurate airplane fuel consumption models [7], [8]. In addition, aircraft manufacturers can often provide much more accurate performance data, which is utilized by pilots to perform flight planning.

Second, the fuel consumption model requires quality inputs to generate meaningful fuel requirements. Some important model inputs are payload, alternate airport, and the flight route [9]. Payload estimation is based on regular booking update, recent statistical data on people and luggage weights. The selection of alternate airport is based on visibility and landing capability at the destination airport. The most interesting input that attracts a lot of research attention is route selection. Route selection is based on waypoints called Very High Frequency Omnidirectional Range (VOR) and airways [9]. The available algorithms can be divided into two categories. In the first category, the path is unknown and solved as a waypoint sequence [10], [11]. In [10], the optimal waypoint sequences with timestamps are computed by a set of prioritized and decentralized path planning problems, with weather and dynamic constraints. In [11], the optimal trajectory is computed from a Multiphase Mixed-Integer Program (MultiMIP), with wind and dynamic constraints. In the second category, the path is predefined as a VOR sequence and airway segments. The goal is to control the aircraft speed or switch modes to resolve congestions or conflicts. This field is known as Traffic Flow Management (TFM). In TFM, researchers have tried hybrid optimal control [12], [13], singular control [14], [15], multistage nonlinear programming [16], and network-model-based optimal control [17], [18]. Most of these methods are computationally expensive, and are only suitable for a small number of nodes (VORs) at the airborne stage.

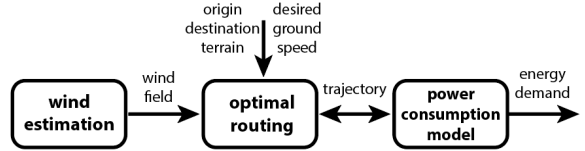
### III. PROPOSED UTM FLIGHT PLANNING SYSTEM

In this paper, we would like to explore a similar energy-based flight planning scheme for UTM. To put the problem into context, we focus on a package delivery example similar to Amazon Prime Air [19]. The goal is to ensure that a multirotor sUAS has enough energy to fly from an origin to a destination optimally under the influence of wind.

The proposed flight planning system diagram is shown in Figure 1. Figure 1a shows the decision diagram with inputs as energy demand and capacity, and output as a vehicle-battery combination. In our example, the energy capacity is simply the battery capacity. Unlike manned aircraft, a multirotor sUAS typically uses Lithium Polymer (LiPo) batteries as the energy source. Due to size and payload limitations, there are only a discrete number of choices available for a given vehicle. And the battery weight usually accounts for a significant portion



(a) The decision diagram.



(b) The energy demand computation flow.

Fig. 1. The proposed system diagram for UTM flight planning.

of the vehicle weight. Assume that the energy demands are known for different LiPo batteries, then the feasible vehicle-battery combinations are the ones with demand-capacity ratios less than 1.0. A combination with demand-capacity ratio close to 1.0 is efficient but risky. Some contingency capacity should be reserved for unexpected situations.

Similar to general aviation, the challenge is to compute a good energy demand estimate, we propose a work flow similar to aviation (Figure 1b). The process is best-understood in a backward sequence. First, we need a vehicle-specific power consumption model to account for different energy components (Section IV). In our example, we focus on multirotor type of sUAS because they are capable of vertical-take-off-and-landing and advantageous in urban environments.

Second, we need an algorithm to perform energy-based optimal routing (Section V). Unlike general aviation, in which the routes are mostly given by a small set of nodes (VORs or airports) and edges (airways), it is impossible to assume such infrastructure in UTM for two reasons. First, to account for terrain complexity and static obstacles, the vehicle trajectory has to be much more refined for safety considerations. Second, every home or store could become future UTM “airports”, the number of waypoints will thus grow significantly. Therefore, before we can talk about the traffic flow problem, we have to first solve the autonomous navigation problem for a large set of nodes, which is essentially a path planning problem in robotics.

Lastly, for this approach to be practical, we need to estimate the wind field in the region relevant to the flight mission (Section VI). We only propose an approach to achieve this. The experimental validation is left as future work.

### IV. POWER CONSUMPTION MODEL

In this section, we briefly review existing power consumption models for a multirotor sUAS. Then, we propose a more comprehensive model from the helicopter literature. The model is identified by simple experiments.

## A. Literature Review

Quadrotor is the most common type of multirotor sUAS. Extensive literature has developed in modeling and controlling a quadrotor. Unfortunately, the power consumption problem is not as well-studied. In [20], the power consumption of multirotors with different number of rotors was studied experimentally. In [21], power consumption of motors was studied as a function of thrust. But in both cases, no systematic models were developed. In [22], a detailed power consumption model was developed for a convertible vertical-take-off-and-landing (VTOL) sUAS, but it is not for multirotor type of vehicles. Multirotors are one type of helicopters. Therefore, it makes sense to review the well-developed helicopter power consumption literature [23], [24]. The proposed model is based mostly on [23].

## B. Proposed Model

The proposed power consumption model consists of three components, namely induced power ( $P_i$ ), profile power ( $P_p$ ), and parasite power ( $P_{par}$ ). The induced power produces the thrust by propelling air downward. The profile power overcomes the rotational drag encountered by rotating propeller blades. The parasite power resists translational body drag when there is relative motion between the vehicle and wind. Detailed derivation based on first principles is addressed in a separate paper. Interested readers can refer to [23]. If we assume that wind is horizontal, then a simplified summary of the model is as follows.

$$\begin{aligned} P_i(T, V_{vert}) &= k_1 T \left[ \frac{V_{vert}}{2} + \sqrt{\left(\frac{V_{vert}}{2}\right)^2 + \frac{T}{k_2}} \right] \\ P_p(T) &= \alpha_2 T^{3/2} \\ P_{par}(\mathbf{V}_{air}) &= \alpha_3 \|\mathbf{V}_{air}\|^3 = \alpha_3 \|\mathbf{V}_{ground} - \mathbf{V}_{wind}\|^3 \end{aligned} \quad (1)$$

where

- $T$  is the total thrust.
- $V_{vert}$  is the vertical speed.
- $\mathbf{V}_{air}, \mathbf{V}_{ground}, \mathbf{V}_{wind}$  are the horizontal air velocity, ground velocity, and wind velocity, respectively.
- $k_1, k_2, \alpha_2, \alpha_3$  are constants to be identified in experiments.

When hovering ( $V_{vert} = 0$ ), the induced power is reduced to

$$P_{i,hover}(T) = \frac{k_1}{k_2} T^{3/2} \triangleq \alpha_1 T^{3/2} \quad (2)$$

For a typical helicopter, The three power components accounts for more than 95% of the total power consumption [23]. The model should be equally valid to a multirotor as long as the vehicle has no rotor interference, which is valid for a typical quadrotor because the propeller disks are not overlapping [23]. The question is how much each individual power component contributes to the total power, which we address in Section IV-C.

TABLE I  
IDENTIFIED PARAMETERS FROM EXPERIMENT

parameter	value
$k_1$	0.8554
$k_2$	$0.3051(kg/m)^{1/2}$
$\alpha_1 = k_1/k_2$	$2.8037(m/kg)^{1/2}$
$\alpha_2$	$0.3177(m/kg)^{1/2}$

## C. Model Identification by Experiments

From equation (1) and (2), the power components are superlinear functions of payload and wind. Thus, we will focus on these two important factors in this section. To identify the unknown coefficients, we performed three simple experiments, namely hover, steady-state ascend/descend, and steady-state circle, on an IRIS+ from 3D Robotics [25] with a self weight of  $m.g = 1.43kg$ . To minimize the effect of wind, the experiments were performed in a football field surrounded by plants on two sides. The detail identification process is documented in a separate paper.

The identified parameters are shown in Table I. Note that the parameter  $\alpha_3$  cannot be identified due to the complication of wind. Specifically, we cannot obtain steady-state readings of  $V_{air}$  when the vehicle is circling. In addition, the geometry of the payload also affects the circling paths. Figure 2 shows the paths when the vehicle is with and without a package payload. We will leave this part as future work.

## V. OPTIMAL ROUTING

In this section, we first review path planning algorithms in the robotics literature. Then we apply fast marching method (FMM) and ordered upwind method (OUM) to UTM optimal routing. The main contribution is on combining the algorithms with energy-based cost profiles derived from the power model in Section IV.

### A. Literature Review

Many research efforts have focused on UAS path planning [26], [27]. In [28] and [29], the problem was formulated as a Mixed-Integer Program with rectangular constraints for static obstacles. However, this approach is computationally intensive. A second approach is potential field [30], which is computationally fast but non-optimal and incomplete, or no guarantee to reach the destination. Another type of approach is heuristic-based such as A\* and D\* [31]. These algorithms are fast but non-optimal. In addition, we have the Dijkstra's algorithm [32], which produces optimal paths in graphs.

The algorithms of choice are variants of the Dijkstra's algorithm designed for wave front propagation on surfaces. An example is the fast marching method (FMM) [33]. It improves the cost update in the Dijkstra's algorithm to achieve optimality in continuum, but FMM cannot take into account the effect of wind. To resolve this issue, another variant of the Dijkstra's algorithm called the ordered upwind method (OUM) is adopted [34]. But OUM is computationally slower

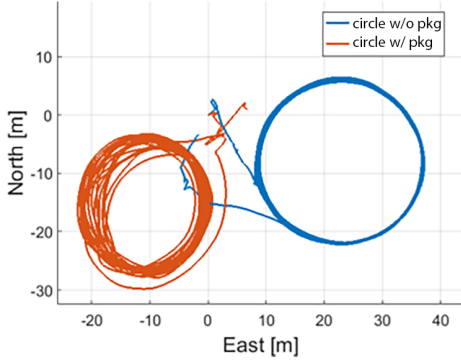


Fig. 2. Experiment 3: Circling path comparison for an IRIS+ with and without the empty package.

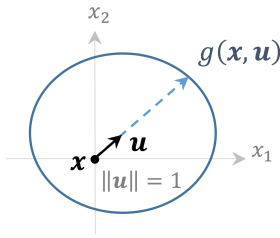


Fig. 3. 2D visualization of the cost profile set  $CP(\mathbf{x}, \mathbf{u})$ .

than FMM by a constant factor. Therefore, when wind is insignificant, FMM is still the best choice.

### B. Algorithm Design in UTM Context

In this section, we discuss the data structure to represent the world and the cost profiles to perform FMM and OUM. Due to space limitation, we skip reviewing the details of the algorithms. Interested readers may refer to [33] for FMM and [34] for OUM.

1) *World Representation*: To account for static obstructions such as terrain and buildings, we run the algorithms on digital elevation models (DEM) [35]. DEM is simply a triangulated mesh data structure with lists of vertices, edges, and faces. Large scale terrain DEM can be obtained from NASA ASTER GDEM2 [36].

For UTM routing, we elevate the DEM model upward by  $150m$  ( $500ft$ ), and then smooth it to avoid sharp change in altitude. The resulting mesh is a 2D surface on which we perform the routing computation.

2) *Cost Profile Design*: Imagine a quadrotor flying at position  $\mathbf{x}$  is influenced by wind velocity  $\mathbf{V}_{wind}(\mathbf{x})$ . Depending on which direction it is heading, the energy consumption, or cost, will be different. This behavior is captured by the cost profile.

We define the cost profile set in equation (3). It is a set of vectors with different magnitudes  $g(\mathbf{x}, \mathbf{u})$  depending on which direction  $\mathbf{u}$  we are heading at position  $\mathbf{x}$ . Figure 3 illustrates the cost profile concept in 2D.

$$CP(\mathbf{x}, \mathbf{u}) = \{\mathbf{u} \cdot g(\mathbf{x}, \mathbf{u}) \mid \mathbf{x} \in \mathbb{R}^n, \mathbf{u} \in \mathcal{U}\} \quad (3)$$

If the cost profile is a circle centered at  $\mathbf{x}$ , then we say the cost is isotropic. In this case, the effect of wind is negligible, and the optimal routing problem can be solved efficient by FMM. Otherwise, the cost is anisotropic, and the effect of wind is noticeable. In this case, OUM is the method of choice.

The remaining task is to specify the cost profile  $g(\mathbf{x}, \mathbf{u})$ . The control direction  $\mathbf{u}$  is a unit vector pointing in the direction of the ground velocity  $\mathbf{V}_{ground}$ . When parasite power is negligible, the cost is independent of control direction  $\mathbf{u}$  (isotropic), and the total cost  $J(\mathbf{x})$  can be solved numerically by FMM. Then at the cruising stage, the cost profile is defined by equation (4).

$$g_{fmm}(\mathbf{x}) = (P_i + P_p)/V_{ground}(\mathbf{x}) \quad (4)$$

When parasite drag is significant, the cost profile is dependent on direction  $\mathbf{u}$  (anisotropic), and the total cost  $J(\mathbf{x})$  can be solved numerically by OUM. At the cruising stage, the cost profile is defined by equation (5). The parasite power is a function of air velocity  $\mathbf{V}_{air}$  (equation (1)), and thus depends on both position  $\mathbf{x}$ , or  $\mathbf{V}_{wind}$ , and control  $\mathbf{u}$ , or the direction of  $\mathbf{V}_{ground}$ . Lastly, for safety considerations, we impose infinite cost on regions with wind speed exceeding a maximum threshold  $V_{wind,max}$ , so that the optimal path does not enter these regions.

$$g_{oum}(\mathbf{x}, \mathbf{u}) = (P_i + P_p + P_{par}(\mathbf{x}, \mathbf{u}))/V_{ground}(\mathbf{x}) + I_{inf}(\|\mathbf{V}_{wind}(\mathbf{x})\| > V_{wind,max}) \quad (5)$$

where the function  $I_{inf}(\cdot)$  is defined as

$$I_{inf}(\text{condition}) = \begin{cases} \infty, & \text{if condition is true} \\ 0, & \text{otherwise} \end{cases} \quad (6)$$

After running the routing algorithm, the optimal cost map is in unit of *Joule* [ $J$ ], or more commonly *mAh* for a LiPo battery with fixed number of cells. This is the minimum energy required to reach the destination at the cruising stage. Then, we can further include the energy consumed during take-off and landing to obtain the estimated energy consumed in the entire trip. Other contingency-related energy considerations can be applied on top of the energy estimate to obtain the total energy demand.

The optimal path is found by running gradient descent from the desired destination [33], and the 4D trajectory with time stamps is obtained by combining the position  $\mathbf{x}$  and ground velocity  $\mathbf{V}_{ground}(\mathbf{x})$  along the 3D path.

Lastly, traffic flow management (TFM) techniques can be applied to introduce delay controls to multiple trajectories in the same airspace, to optimize operational and policy constraints [12]–[18]. This is left as a future research topic.

### C. Simulations

In this section, routing examples are provided in simulation. The energy cost are computed numerically from equation (??), (4), and (5), using the parameters in Table I and a ground speed  $V_{ground} = 10m/s$ . For illustration purpose, the parameter  $\alpha_3$  is approximated to be  $0.1kg/m$  from [37].

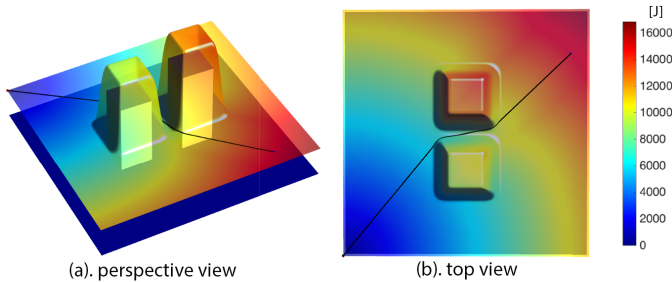


Fig. 4. FMM computation results on optimal costs and paths with static obstacles.

1) *FMM without wind*: Figure 4 shows an optimal routing example using FMM on a  $250m \times 300m$  space with two building obstructions. The origin is at the lower-left corner from the top view, while the destination is close to the upper-right corner. The cost profile takes into account induced and profile power, and the optimal cost, or minimum energy, to destination is about  $1.4 \times 10^4 J$ . From Table I, if the vehicle flies at  $150m$  altitude, the energy spent on ascend and descend at  $2.5m/s$  is  $1.98 \times 10^4 J$ . The total energy spent on the trip is  $3.38 \times 10^4 J$ , or  $782mAh$  with a  $12V$  3-cell LiPo battery.

2) *OUM with wind*: To observe the effect of wind, we performed OUM simulations on a  $1000m \times 1000m$  flat surface. 3D surfaces are possible but not presented. The result is shown in Figure 5. Figure 5a shows a randomized wind field with main direction heading  $45^\circ$  to the  $+x$ -axis, and with wind speed ranging from  $0$  to  $5m/s$ , which yields comparable parasite drag. The sUAS goes from the origin to the lower-left corner  $(-500m, 500m)$ .

Figure 5b shows the result with parasite power only, with minimum energy of  $1.03 \times 10^4 J$ . The wind field is overlaid as reference. Figure 5c shows the result with induced power and profile power. They are constant throughout the navigation, so the optimal cost are symmetric rings around the origin. It takes  $1.14 \times 10^4 J$  to destination. The same result can be obtained faster via FMM. With all power components (Figure 5d), the optimal route is somewhere in between the previous two cases, and the minimum energy is  $2.37 \times 10^4 J$ . The value is larger than the sum of the previous two cases because the route is longer than the one in Figure 5c. Lastly, by including the  $1.98 \times 10^4 J$  energy consumed during take-off and landing at  $150m$  altitude with  $2.5m/s$  vertical speed, we obtain the total energy  $4.35 \times 10^4 J$ , or  $1010mAh$  for a  $12V$  3-cell LiPo battery.

For validation, we can perform a simple thought experiment for the above scenario. The ascend and descend phases takes  $1min$  each to complete, and the flying phase takes about  $1.3min$ . Therefore, the vehicle spent  $1010mAh$  in  $3.3min$ . With the  $5100mAh$  default LiPo battery, the IRIS+ sUAS can operate for about  $17min$ . This duration is confirmed repeatedly in our testings under nominal conditions.

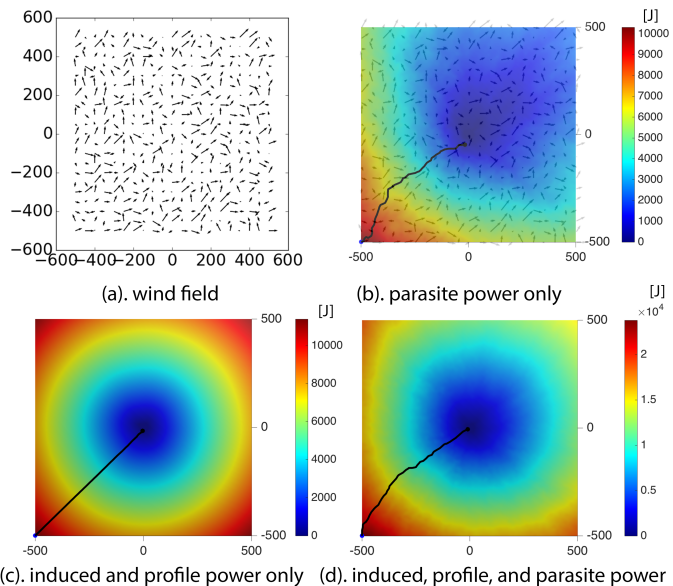


Fig. 5. OUM computation results on optimal costs and paths with different energy components.

## VI. WIND ESTIMATION

One of the biggest challenges in UTM is the lack of wind and weather data [2] in the low-altitude Class G airspace. In this section, we would like to review existing wind data collection technologies and propose a complementary wind estimation method for UTM.

Wind data at the boundary layer, or low-altitude airspace, is commonly collected with radar or sodar-based wind profilers [38], [39]. Currently, the best available wind forecast data is from the High-Resolution Rapid Refresh (HRRR) radar assimilation [40]. However, due to terrain geometry, the wind behavior at low altitude is quite complicated. Studies have conducted on verifying the accuracy of HRRR [41], but the result does not seem good. In addition, the infrastructure required for data collection is cumbersome and expensive.

To complement with the existing wind forecast system, we propose to use sUAS as distributed sensors to measure wind fields in real time. Each sUAS can broadcast its time stamp, position, and estimated wind vector via Automatic Dependent Surveillance-Broadcast (ADS-B) [42], so that an sUAS in mission has the latest wind information around it. There is a rich literature on fixed-wing sUAS wind estimation with pitot tubes and Extended Kalman Filters (EKF) [43] or vehicle kinematics [44]. In [37], the wind speed and direction is estimated by a hovering quadrotor without any atmospheric wind measurement sensor. Lastly, wind tunnel testings were performed in [45] to characterize the effect of wind, and the drag coefficient seems to be a strong function of yaw.

However, this approach requires a minimum vehicle density to become useful. Based on the Metropolis study [46], we envision the future UTM will eventually overcome this barrier. A small scale demonstration is left as future work.

## VII. CONCLUSION

In summary, we proposed an energy-based flight planning system for UTM. The system is designed to mimic the fuel loading process in ATM flight planning. The main challenge is on computing the energy demand. To resolve this, we break the demand problem into three solvable small problems, and introduced them in a backward sequence. First, a power consumption model is proposed for energy estimation. Second, routing algorithms such as FMM and OUM provide the optimal paths. Since the algorithms are capable of optimizing energy consumption, we proposed energy-based cost profiles to perform optimal routing. The advantage is that the algorithm gives the energy consumption directly. A future research direction can be combining the optimal routing algorithm with TFM algorithms for multi-aircraft regulation. Finally, we proposed a wind estimation procedure to complement the existing wind data collection infrastructure. The validity is to be confirmed in future.

## REFERENCES

- [1] "Operation and Certification of Small Unmanned Aircraft Systems." Federal Aviation Administration, 2015, 14 CFR Parts 21, 43, 45, 47, 61, 91, 101, 107, and 183.
- [2] P. H. Kopardekar, "Unmanned aerial system (uas) traffic management (utm): Enabling low-altitude airspace and uas operations," 2014.
- [3] P. Kopardekar, "Safely Enabling Low-Altitude Airspace Operations: Unmanned Aerial System Traffic Management (UTM)," 2015.
- [4] M. S. Ryerson, M. Hansen, L. Hao, and M. Seelhorst, "Landing on empty: estimating the benefits from reducing fuel uplift in us civil aviation," *Environmental Research Letters*, vol. 10, no. 9, p. 094002, 2015.
- [5] M. S. Ryerson, M. Hansen, and J. Bonn, "Fuel consumption and operational performance," *Transportation Research*, no. Part D, pp. 305–314, 2011.
- [6] International Civil Aviation Organization, ICAO Engine Exhaust Emissions Data, Doc 9646-AN/943, Tech. Rep., 2005.
- [7] D. A. Senzig, G. G. Fleming, and R. J. Iovinelli, "Modeling of terminal-area airplane fuel consumption," *Journal of Aircraft*, vol. 46, no. 4, pp. 1089–1093, 2009.
- [8] D. Senzig, G. Fleming, and R. Iovinelli, "Fuel consumption modeling in support of atm environmental decision-making," in *Proceedings of the Eighth Annual FAA/EUROCONTROL Air Traffic Management Research and Development Seminar, Napa, CA*, 2009.
- [9] M. Nolan, *Fundamentals of air traffic control*. Cengage learning, 2010.
- [10] W. Zhang, M. Kamgarpour, D. Sun, and C. J. Tomlin, "A hierarchical flight planning framework for air traffic management," *Proceedings of the IEEE*, vol. 100, no. 1, pp. 179–194, 2012.
- [11] M. Soler, *Commercial aircraft trajectory planning based on multiphase mixed-integer optimal control*. Omm Editorial, 2013.
- [12] M. Soler, A. Olivares, and E. Staffetti, "Hybrid optimal control approach to commercial aircraft trajectory planning," *Journal of Guidance, Control, and Dynamics*, vol. 33, no. 3, pp. 985–991, 2010.
- [13] M. Soler, A. Olivares, E. Staffetti, and D. Zapata, "Framework for aircraft trajectory planning toward an efficient air traffic management," *Journal of Aircraft*, vol. 49, no. 1, pp. 341–348, 2012.
- [14] D. M. Pargett and M. D. Ardema, "Flight path optimization at constant altitude," *Journal of guidance, control, and dynamics*, vol. 30, no. 4, pp. 1197–1201, 2007.
- [15] A. Franco, D. Rivas, and A. Valenzuela, "Minimum-fuel cruise at constant altitude with fixed arrival time," *Journal of guidance, control, and dynamics*, vol. 33, no. 1, pp. 280–285, 2010.
- [16] M. Jacobsen and U. T. Ringertz, "Airspace constraints in aircraft emission trajectory optimization," *Journal of Aircraft*, vol. 47, no. 4, pp. 1256–1265, 2010.
- [17] H. Huang and C. J. Tomlin, "A network-based approach to en-route sector aircraft trajectory planning," in *AIAA Guidance, Navigation and Control Conference*, 2009.
- [18] D. Sun, S. D. Yang, I. Strub, A. M. Bayen, B. Sridhar, and K. Sheth, "Eulerian trilogy," in *AIAA Guidance, Navigation, and Control Conference and Exhibit*, 2006, p. 6227.
- [19] Determining Safe Access with a Best Equipped, Best-Served Model for Small Unmanned Aircraft Systems. (Date last accessed 14-October-2016). [Online]. Available: [http://utm.arc.nasa.gov/docs/Amazon\\_Determining%20Safe%20Access%20with%20a%20Best-Equipped,%20Best-Served%20Model%20for%20sUAS\[2\].pdf](http://utm.arc.nasa.gov/docs/Amazon_Determining%20Safe%20Access%20with%20a%20Best-Equipped,%20Best-Served%20Model%20for%20sUAS[2].pdf)
- [20] D. Aleksandrov and I. Penkov, "Energy consumption of mini uav helicopters with different number of rotors," in *11th International Symposium "Topical Problems in the Field of Electrical and Power Engineering"*, 2012, pp. 259–262.
- [21] Y. Mulgaonkar, M. Whitzer, B. Morgan, C. M. Kroninger, A. M. Harrington, and V. Kumar, "Power and weight considerations in small, agile quadrotors," in *SPIE Defense+ Security*. International Society for Optics and Photonics, 2014, pp. 90 831Q–90 831Q.
- [22] D.-K. Phung and P. Morin, "Modeling and energy evaluation of small convertible uavs," *IFAC Proceedings Volumes*, vol. 46, no. 30, pp. 212–219, 2013.
- [23] W. Johnson, *Helicopter theory*. Courier Corporation, 2012.
- [24] G. J. Leishman, *Principles of helicopter aerodynamics with CD extra*. Cambridge university press, 2006.
- [25] 3D Robotics IRIS+. (Date last accessed 14-October-2016). [Online]. Available: <http://3dr.com/support/articles/207358106/iris/>
- [26] C. Goerzen, Z. Kong, and B. Mettler, "A survey of motion planning algorithms from the perspective of autonomous uav guidance," *Journal of Intelligent and Robotic Systems*, vol. 57, no. 1-4, pp. 65–100, 2010.
- [27] N. Dadkhah and B. Mettler, "Survey of motion planning literature in the presence of uncertainty: considerations for uav guidance," *Journal of Intelligent & Robotic Systems*, vol. 65, no. 1-4, pp. 233–246, 2012.
- [28] D. Mellinger, A. Kushleyev, and V. Kumar, "Mixed-integer quadratic program trajectory generation for heterogeneous quadrotor teams," in *Robotics and Automation (ICRA), 2012 IEEE International Conference on*. IEEE, 2012, pp. 477–483.
- [29] T. Schouwenaars, B. De Moor, E. Feron, and J. How, "Mixed integer programming for multi-vehicle path planning," in *Control Conference (ECC), 2001 European*. IEEE, 2001, pp. 2603–2608.
- [30] Y. K. Hwang and N. Ahuja, "A potential field approach to path planning," *IEEE Transactions on Robotics and Automation*, vol. 8, no. 1, pp. 23–32, 1992.
- [31] D. Ferguson, M. Likhachev, and A. Stentz, "A guide to heuristic-based path planning," in *Proceedings of the international workshop on planning under uncertainty for autonomous systems, international conference on automated planning and scheduling (ICAPS)*, 2005, pp. 9–18.
- [32] S. Skiena, "Dijkstras algorithm," *Implementing Discrete Mathematics: Combinatorics and Graph Theory with Mathematica*, Reading, MA: Addison-Wesley, pp. 225–227, 1990.
- [33] J. A. Sethian, "Fast marching methods," *SIAM review*, vol. 41, no. 2, pp. 199–235, 1999.
- [34] J. A. Sethian and A. Vladimirsky, "Ordered upwind methods for static hamilton-jacobi equations: Theory and algorithms," *SIAM Journal on Numerical Analysis*, vol. 41, no. 1, pp. 325–363, 2003.
- [35] D. F. Maune, *Digital elevation model technologies and applications: the DEM users manual*. Asprs Publications, 2007.
- [36] NASA DEM Models. (Date last accessed 14-October-2016). [Online]. Available: [https://lpdaac.usgs.gov/dataset\\_discovery/aster/aster\\_products\\_table/ast14dem](https://lpdaac.usgs.gov/dataset_discovery/aster/aster_products_table/ast14dem)
- [37] J. Moyano Cano, "Quadrotor uav for wind profile characterization," 2013.
- [38] W. L. Ecklund, D. A. Carter, and B. B. Balsley, "A uhf wind profiler for the boundary layer: Brief description and initial results," *Journal of Atmospheric and Oceanic Technology*, vol. 5, no. 3, pp. 432–441, 1988.
- [39] F. Ralph, C. Mazaudier, M. Crochet, and S. Venkateswaran, "Doppler sodar and radar wind-profiler observations of gravity-wave activity associated with a gravity current," *Monthly weather review*, vol. 121, no. 2, pp. 444–463, 1993.
- [40] T. L. Smith, S. Benjamin, J. Brown, S. Weygandt, T. Smirnova, and B. Schwartz, "Convection forecasts from the hourly updated, 3-km high resolution rapid refresh model," in *Preprints, 24th Conf. on Severe Local Storms, Savannah, GA, Amer. Meteor. Soc.*, vol. 11, 2008.
- [41] Wind Decision Support for UAS Operations, NASA Weather Workshop. (Date last accessed 14-October-2016). [Online]. Avail-

able: [http://aviationsystems.arc.nasa.gov/utm-weather/presentations/9\\_2016\\_Evans\\_UTM%20Weather\\_Workshop\\_V3.1.pdf](http://aviationsystems.arc.nasa.gov/utm-weather/presentations/9_2016_Evans_UTM%20Weather_Workshop_V3.1.pdf)

- [42] R. T. C. for Aeronautics, *Minimum Aviation System Performance Standards for Automatic Dependent Surveillance Broadcast (ADS-S)*. RTCA, Incorporated, 2002.
- [43] A. Cho, J. Kim, S. Lee, and C. Kee, "Wind estimation and airspeed calibration using a uav with a single-antenna gps receiver and pitot tube," *IEEE transactions on aerospace and electronic systems*, vol. 47, no. 1, pp. 109–117, 2011.
- [44] J. W. Langelaan, N. Alley, and J. Neidhoefer, "Wind field estimation for small unmanned aerial vehicles," *Journal of Guidance, Control, and Dynamics*, vol. 34, no. 4, pp. 1016–1030, 2011.
- [45] F. Schiano, J. Alonso-Mora, K. Rudin, P. Beardsley, R. Siegwart, and B. Siciliano, "Towards estimation and correction of wind effects on a quadrotor uav," in *IMAV 2014: International Micro Air Vehicle Conference and Competition 2014, Delft, The Netherlands, August 12-15, 2014*. Delft University of Technology, 2014.
- [46] E. Sunil, J. Hoekstra, J. Ellerbroek, F. Bussink, D. Nieuwenhuisen, A. Vidosavljevic, and S. Kern, "Metropolis: Relating airspace structure and capacity for extreme traffic densities," in *ATM seminar 2015, 11th USA/EUROPE Air Traffic Management R&D Seminar*, 2015.